A closer look at the mathematical model of a cryogenic current comparator

V C de Oliveira, R P Landim and C B Prado

Instituto Nacional de Metrologia, Qualidade e Tecnologia (INMETRO), Av. Nossa Senhora das Graças, 50, Xerém, Duque de Caxias - RJ - Brazil

vcoutinho@inmetro.gov.br

Abstract. A virtual resistor is a hardware and software assembly that realizes a control system to emulate "traditional" resistive components without the loss of energy efficiency that they entail. There are possible applications for virtual resistors to the Metrology in Electrical Resistance Standardization. However, as in any control system analysis, it is necessary to build proper mathematical models. Hence, a white-box modeling approach is required to understand the physical phenomena that affect the variability of measurements performed with resistance comparator bridges. This paper discusses how to start building a mathematical model for a resistance comparator bridge based on a commercial cryogenic current comparator. The data collection and statistical analyses necessary for refining such a model are presented. Results indicate that the current values along a measurement do not always fit a normal distribution. Moreover, there are some cases where one cannot assume that the current value is constant over the measurement period, i.e., there is a noticeable trend for current drift.

1. Introduction

The INMETRO has an ongoing project that aims at the development and metrological characterization of a programmable virtual resistor – in the sense that the system's operator can program the nominal value of such resistor – and the evaluation of its application as a direct current (dc) electrical resistance standard, alternatively to conventional standards like precision resistors (with fixed values), resistance decade boxes, and multifunction calibrators.

A virtual resistor is a hardware and software assembly that realizes a control system to emulate "traditional" resistive components without the loss of energy efficiency that they entail. The concept and implementation of virtual resistors originate from the Electrical Power Systems and Industrial Electronics, Electronic Systems, and Controls expertise fields. The first publication to deal with virtual resistors [1] proposed a method to dampen transient oscillations on the output filter of Pulse Width Modulation (PWM) inverters using a virtual resistor instead of a "real" resistor.

Nonetheless, most investigations focus on alternating current (ac) implementations of virtual resistors based on typical parameters of dc-ac conversion systems, in contrast to the dc modeling sought by this project. Besides, these investigations neither assess the application of virtual resistors to the Metrology in Electrical Resistance Standardization nor contemplate certain important metrological aspects such as uncertainties, stability, and operating range.

Building adequate mathematical models is the first and most crucial step in the control systems

analysis as a whole [2]. Therefore, in the starting stages of the project, the objective is to develop mathematical models of resistance comparator bridges that will later allow the integration with the mathematical model of the virtual resistor instead of a conventional artifact.

In general, calibration laboratories adopt black-box or gray-box modeling approaches [3] for their measurement systems because they do not have or do not need a complete knowledge of these. However, this project requires a white-box modeling approach [3] due to the need to understand the physical phenomena that influence the variability of measurements performed with resistance comparator bridges. Furthermore, since the first stages of the project are just theoretical, it is not possible to identify the relationships between the inputs and outputs of the system (such as those required by black-box and gray-box modeling) from data collection.

In this research, the mathematical description of the physical phenomena that influence the variability of electrical resistance measurement systems originates from the very model equations that traditionally describe them. These equations are understood as sufficiently characterized (e.g., in papers, books, or operating procedures) gray or black-boxes. The "opening" of these boxes carried out in this research is based on technical literature describing the associated physical phenomena and, in addition, on the collection of experimental data. Moreover, whenever the performance evaluation of a model is applicable, it is validated through simulation. Tools like the Uncertainty Machine of the National Institute of Standards and Technology (NIST) [4][5] are convenient for such simulations; still, they do require the probability distributions of the input variables to be specified.

The basis for the pilot study of the mathematical modeling presented in this paper is the cryogenic current comparator (CCC) developed by the National Physical Laboratory (NPL) [6][7] and available in the Quantum Electrical Metrology Laboratory of the INMETRO. It turns out that not all probability distributions of the variables in the CCC model equations are known. Thus, measurement data were collected so that such distributions could be characterized. Details of the CCC, the data collection through measurements, the statistical analyses that led to the characterization of the probability distributions, and the results obtained so far are discussed in the following sections.

2. Materials and methods

2.1. The cryogenic current comparator (CCC)

The CCC is a bridge circuit that measures the ratio of two resistors R_1 and R_2 as a function of a ratio of two currents. Figure 1 shows the CCC scheme used in this work. The current source on the master side applies the current I_1 to the resistor R_1 and the master winding, configured with N_1 turns. The current source on the slave side applies the current I_2 to the resistor R_2 and the slave winding, configured with N_2 turns. The number of turns of the windings is set up using the respective selection switches. The ratio I_1/I_2 between the nominal values of the currents is reciprocal to the ratio R_1/R_2 between the nominal values of the resistors, and N_1/N_2 is equivalent to R_1/R_2; for example, if R_1 = 100 Ω and R_2 = 10 kΩ, I_1 = 3 mA, I_2 = 0.03 mA, N_1 = 8 turns and N_2 = 800 turns.

A null detector based on an A20 nanovoltmeter manufactured by EM Electronics [6] connects the two sides of the CCC. The null detector measures the voltage V_{A20} across the low potential terminals of the resistors. The high potential terminals of the resistors are equipotentialized through a short circuit internal to the CCC. V_{A20} is given by equation (2.1).

$$V_{A20} = I_1 R_1 - I_2 R_2 \tag{2.1}$$

In the balance condition of the bridge, the voltage at the input of A20 is zero. This condition is expressed by equation (2.2).

$$I_1 R_1 - I_2 R_2 = 0 \tag{2.2}$$

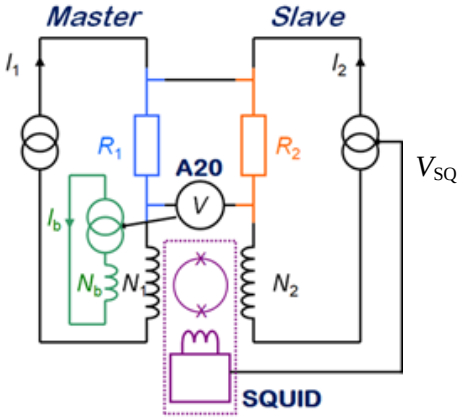

Figure 1. The cryogenic current comparator (CCC) diagram.

The CCC also contains a Superconducting Quantum Interference Device (SQUID), an extremely sensitive magnetic field sensor. Master and slave coils are wound (in opposite directions) on the outer surface of a superconducting toroid [7]. Inside this toroid, there is a pick-up coil connected to the SQUID responsible for detecting minimal differences in magnetic flux resulting from flux imbalance across the master and slave sides (it takes advantage of the superconductor's property of expelling any magnetic field from its interior, the so-called Meissner effect).

The signal V_{SQ} at the SQUID output, proportional to the flux imbalance, is applied to a feedback loop to perform I_2 control, which gives greater accuracy to the measurements with the CCC. V_{SQ} is digitized through a 16-bit analog-to-digital converter (ADC), and the values for I_2 correction are transmitted via an optical fiber interface [8].

To improve accuracy, the CCC includes a second feedback loop that utilizes the voltage signal V_{A20} to command a current source, called balance, through an 18-bit digital-to-analog converter (DAC) [8]. The balance source applies the current I_b to an auxiliary winding known as the balance winding, configured with N_b turns. The balance coil is also wound on the outer surface of the superconducting toroid in the same direction as the slave coil. In the balance condition of the bridge, the flux difference (and hence V_{SQ}) is zero. Equation (2.3) expresses this condition [9].

$$I_1 N_1 - I_2 N_2 - I_b N_b = 0 \tag{2.3}$$

By combining equations (2.2) and (2.3), the ratio between the resistors as a function of the currents I_1 and I_b can be determined, as shown in equation (2.4).

$$\frac{R_1}{R_2} = \frac{N_1}{N_2}\left(1 - \frac{I_b}{I_1}\frac{N_b}{N_1}\right) \tag{2.4}$$

Let us illustrate the CCC controls with examples. Let the flux imbalance Δ_{Flux} be such that $\Delta_{Flux} = I_1N_1 - I_2N_2$ (for simplicity, $N_b = 0$, i.e., the balance coil is short-circuited via its selector switch). If I_1 rises, the flux on the master side, given by I_1N_1, also rises, causing a proportional increase in V_{SQ}. In this case, the V_{SQ} signal corresponds to a command to raise I_2. Consequently, the flux in the slave side (given by I_2N_2) increases until the balance is reached, that is, $I_1N_1 = I_2N_2$ and $V_{SQ} = 0$.

Let us consider a situation where the value of one of the resistors is not exactly equal to its nominal value. Say R_1 = 100.000 Ω, R_2 = 99.990 Ω, I_1 = 3.00000 mA, $N_1 = N_2$ = 32 and N_b = 1. From equation (2.4), the value of I_b results in –9.6 μA. Let the initial value of I_2 be 3.00000 mA; in this case, the SQUID signal corresponds to 9.6 μV instead of zero (equation (2.3)). From this positive signal, a correction value is sent to the slave current source, to adjust I_2 to 3.00030 mA. When applying the adjusted value of I_2 to equations (2.2) and (2.3), it can be seen that this value restores the balance condition of the bridge.

Let us now suppose that, during a measurement round, the value of R_2 shows a change to 99.995 Ω.

From equation (2.4), I_b is –4.8 μA, and the SQUID signal equals to 4.8 μV. The balance condition of the bridge balance is restored thanks to the control action, which adjusts I_2 to 3.00015 mA. Therefore, fluctuations in resistor values throughout a measurement (as well as other fluctuations inherent to the system) reflect in I_b.

In practice, the ratio between resistors R_1/R_2 (henceforth called r) is calculated using equation (2.5),

$$r = \frac{N_1}{N_2}(1 - \delta) \tag{2.5}$$

where δ is described by equation (2.6):

$$\delta = \frac{N_b}{N_1}\frac{I_b}{I_1}F_{cal} \tag{2.6}$$

I_b actually results from a voltage-to-current conversion in which the output voltage of the voltage-current converter (i.e., the balance voltage, V_b) is applied to the 1 MΩ resistor R_b present in the balance circuit (R_b is omitted in figure 1 for the sake of simplicity). F_{cal} corresponds to the product gR_b, where g is the transconductance of the voltage-to-current converter. The converter's input voltage is the command voltage coming from the A20 module. Typical values of F_{cal} are close to 1. To account for the drift of the electronic components involved, F_{cal} must be determined periodically (for example, once a year) in a separate procedure, in which I_b is calibrated against I_1 [6].

The CCC model equation is defined according to equation (2.7) [10]:

$$R_X = r \times R_S \times Z_S \times Z_X \tag{2.7}$$

where R_X is the value of the unknown resistor, which is to be determined by calibrating it against the standard resistor, whose value is known and equal to R_S; Z_S is the R_S correction factor for the pressure and temperature present during the measurement; and Z_X is the factor that converts the R_X value during the measurement to the R_X value under the reference conditions (namely, the reference temperature, T_0, of 23 °C and the reference pressure, P_0, of 101.325 kPa), being given by equation (2.8) [10]:

$$Z_X = 1 - \alpha_{X_{T_0}}(T_X - T_0) - \beta_{X_{T_0}}(T_X - T_0)^2 - \gamma_{X_{P_0}}(P_X - P_0) \tag{2.8}$$

where $\alpha_{X_{T_0}}$ and $\beta_{X_{T_0}}$ are the temperature coefficients (linear and quadratic, respectively) of the said resistor at 23 °C, and $\gamma_{X_{P_0}}$ is the pressure coefficient of the resistor at 101.325 kPa. If T_X (R_X temperature) equals T_0 and P_X (R_X pressure) equals P_0, Z_X equals 1.

2.2. Master current (I_1) measurements

In practice, the CCC program records successive V_b values (i.e., the A20 DAC output voltage) and provides the r values calculated according to equation (2.5) and the definition $I_b = gV_b$. This level of granularity suffices for calibrations performed with the CCC. Yet, it does not allow one to determine how much the standard deviations of I_b and I_1 contribute individually to the standard deviation of r. Besides, the characterization of the probability distribution of I_1 is unknown. This circumstance drove the need to perform measurements of I_1 (with different nominal values) and statistical treatment of data from these measurements.

The CCC's master currents were measured with the aid of an Agilent 3458A multimeter, serial number MY45040453, calibrated on 2022-04-07 by the Electrical Metrology Calibration Laboratory of the INMETRO under certificate number Dimci 0329/2022. The necessary corrections from the certificate were applied to the readings performed by the multimeter. The measurements took place from February to March 2023. The multimeter self-calibration procedure ("ACAL ALL" command) was performed daily and systematically right before the beginning of the measurements. A LabVIEW 2014 program running on a notebook connected to the multimeter through a USB-GPIB (Universal Serial Bus - General Purpose Interface Bus) interface recorded the values read by the multimeter. Environmental conditions were monitored during the measurements.

The master current source was connected directly to the front terminals of the multimeter (dc ammeter function). Measurements were conducted for the five master current values achievable by the CCC: 30 mA, 10 mA, 3 mA, 1 mA, and 0.3 mA [6]. Before the measurement, the nominal current value had to be configured in the "ACB server" program, which runs on the CCC computer and is responsible for commanding the system. The "ACB server" also loads the CCC configuration .ini file, which assigns the gain and offset values to the CCC current source circuits, determined in a separate calibration procedure. In this study, the .ini file utilized was the one respective to the calibration procedure realized in 2023. Each measurement consisted of 25 forward (positive) and 25 reverse (negative) current cycles, with 100 points per cycle, totaling 5000 points per measurement round. The 3458's ADC integration time in terms of power line cycles (i.e., the time during which the ADC measures the input signal, set by the NPLC parameter [11]) was 20, yielding one sample (reading) per second.

3. Results and discussion

In the first analyzed scenario, the 25 positive cycles are treated as a single dataset – likewise, the 25 negative cycles are considered a single dataset, as exemplified by figure 2. For each dataset, the parameters listed in table 1 were calculated. Table 2 summarizes the results for the positive cycles with every nominal value applied. The results for the negative cycles are shown in table 3.

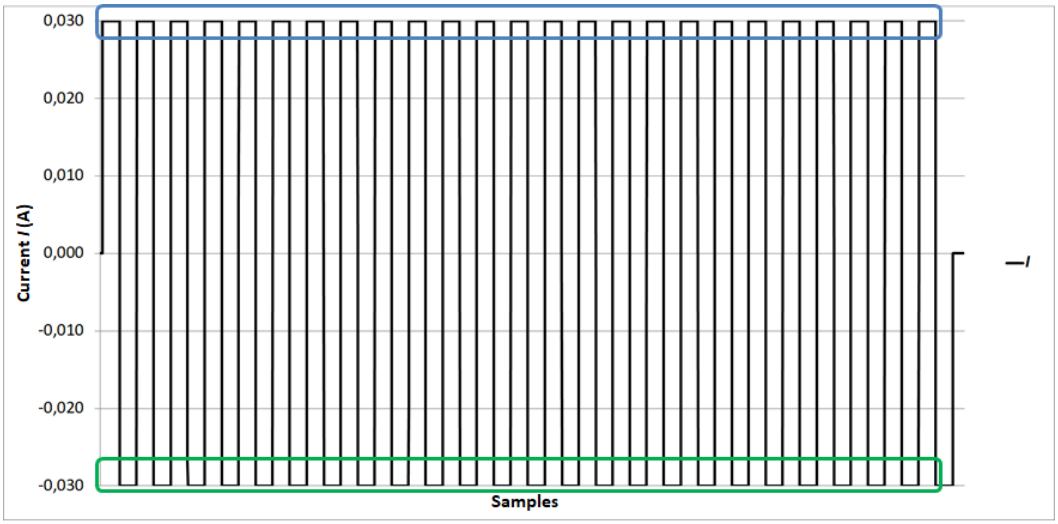

Figure 2. Current cycles applied by the CCC's master current source.

Table 1. Parameters whose values were calculated considering 25 cycles as a single set.

Parameter symbol	Parameter description
μ	Average current value in each measurement
n	Number of samples considered (the values read during the transitions between positive and negative cycles are discarded)
σ	Standard deviation in each measurement
$u_A(I)$	Type A standard uncertainty calculated according to the Guide to the expression of uncertainty in measurement [12], $u_A(I) = \sigma/n^{1/2}$
$u_{A\_rel}(I)$	Relative Type A standard uncertainty
Amplitude	Difference between the maximum and minimum values recorded during the measurement round
$u_B(I)$	Type B standard uncertainty. $u_B(I) = U/k$,where U is the expanded uncertainty of the multimeter and k is the coverage factor, k = 2,00 (U and k given in the certificate)

Table 2. Summary of measurement results considering the 25 positive cycles as a single set.

	I_1 = 30 mA	I_1 = 10 mA	I_1 = 3 mA	I_1 = 1 mA	I_1 = 0.3 mA
3458A range	0.1 A	0.01 A	0.01 A	0.001 A	0.001 A
n	2467	2468	2467	2465	2466
μ	29.9998 mA	10.00004 mA	2.99999 mA	0.999947 mA	0.299985 mA
σ	1.5×10^{-7} A	6.0×10^{-8} A	0.8×10^{-8} A	1.6×10^{-9} A	0.7×10^{-9} A
$u_A(I)$	3.0×10^{-9} A	1.2×10^{-9} A	0.2×10^{-9} A	0.1×10^{-9} A	0.1×10^{-9} A
$u_{A\_rel}(I)$	0.1 μA/A	0.2 μA/A	0.1 μA/A	0.1 μA/A	0.1 μA/A
Amplitude	10.0×10^{-7} A	33.0×10^{-8} A	6.0×10^{-8} A	9.0×10^{-9} A	6.0×10^{-9} A
$u_B(I)$	2.0×10^{-7} A	5.0×10^{-8} A	2.0×10^{-8} A	5.0×10^{-9} A	2.0×10^{-9} A

Table 3. Summary of measurement results considering the 25 negative cycles as a single set.

	I_1 = −30 mA	I_1 = −10 mA	I_1 = −3 mA	I_1 = −1 mA	I_1 = −0.3 mA
3458A range	0.1 A	0.01 A	0.01 A	0.001 A	0.001 A
n	2468	2464	2467	2468	2467
μ	−30.0002 mA	−9.99995 mA	−2.99999 mA	−1.000009 mA	−0.300007 mA
σ	1.2×10^{-7} A	4.1×10^{-8} A	0.8×10^{-8} A	1.3×10^{-9} A	0.7×10^{-9} A
$u_A(I)$	2.4×10^{-9} A	0.9×10^{-9} A	0.2×10^{-9} A	0.1×10^{-9} A	0.1×10^{-9} A
$u_{A\_rel}(I)$	0.1 μA/A	0.1 μA/A	0.1 μA/A	0.1 μA/A	0.1 μA/A
Amplitude	8.0×10^{-7} A	21.0×10^{-8} A	7.0×10^{-8} A	9.0×10^{-9} A	7.0×10^{-9} A
$u_B(I)$	2.0×10^{-7} A	5.0×10^{-8} A	2.0×10^{-8} A	5.0×10^{-9} A	2.0×10^{-9} A

The assumption of normality of these datasets was also tested by running the Shapiro-Wilk Test for normality in R. None of the sets was found to fit the normal distribution, i.e., for every test, the computed p-value was less than 0.05.

Minitab®'s "Individual Distribution Identification" feature was also employed to test the goodness of fit to the exponential, gamma, and Weibull distributions, besides the normal distribution. Still, no distribution was found to be fit (although the Minitab® Statistical Software uses the Anderson-Darling Test, which is less powerful than the Shapiro-Wilk Test [13]).

The Pearson correlation coefficient ρ for the datasets was also calculated to assess the linear correlation between the master current values and time (represented by the samples in ascending order). As a rule, the current value is assumed to remain practically constant over the measurement period. Therefore, this assessment was conducted with the purpose of checking whether this holds true. The results are summarized in table 4, in which the classification of the degree of correlation from "very low" to "very high" follows the described in [14]. The results contradict this common sense; i.e., in some cases, there is a noticeable trend for current drift.

Table 4. Summary of Pearson coefficient (ρ) calculation results, first scenario.

Absolute nominal value	ρ (positive current values)	ρ (negative current values)	Degree of correlation (positive values)	Degree of correlation (negative values)
30 mA	−0.77	−0.71	High	High
10 mA	0.56	0.23	Moderate	Very low
3 mA	−0.14	−0.49	Very low	Low
1 mA	0.58	−0.60	Moderate	Moderate
0.3 mA	−0.04	−0.08	Very low	Very low

In practice, when measuring with the CCC, 10 cycles (5 forward and 5 reverse current cycles) are typically run [15]. However, in the scenario presented above, 50 cycles (25 forward and 25 reverse current cycles) were performed based on the assumption that, as sample size increases, the frequency

distribution converges to a normal distribution. Nevertheless, statistical results rule out the assumption of normality under these conditions.

Therefore, a second scenario was addressed to check for the assumption of normality under usual measurement conditions. Such conditions include discarding the initial 20 s (guard interval) and considering only the subsequent 20 s – as shown in figure 3 – in the first 5 positive and the first 5 negative cycles. This guard interval is necessary because the A20 servo control needs some settling time, since the digital control loops are off during the current reversals [8][15]. In this scenario, each cycle was treated as a single dataset. For each dataset, the Shapiro-Wilk Test for normality was performed in R, and the results are shown in table 5. From the 50 cycles considered, 45 (90 % of the datasets) were fit to the normal distribution. The 5 outliers occasionally fit the exponential or Weibull distribution (according to the results obtained with Minitab), but the general trend indicates that the normal distribution is the most appropriate.

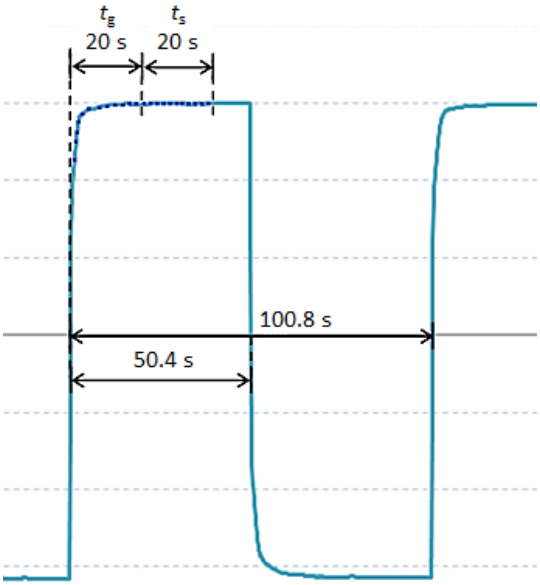

Figure 3. Typical CCC measurement cycle times: t_g is the 20 s guard interval (transition time + wait time), and t_s is the 20 s interval valid for the measurements [15].

Table 5. Number of cycles (out of 5 in each case) fitted to the normal distribution.

Absolute nominal value of I_1	Number of cycles fit to the normal distribution (positive current values)	Number of cycles fit to the normal distribution (negative current values)
30 mA	4	5
10 mA	4	5
3 mA	5	4
1 mA	4	5
0.3 mA	5	4

When the first 5 cycles (discarded the initial 20 s and kept only in the subsequent 20 s) are taken as a single set, the tendency for adequacy to the normal distribution remains, as seen in table 6. W value is the Shapiro-Wilk test statistic (as computed in R). Other possible distributions were checked with the aid of Minitab®. The Pearson correlation coefficient ρ for these datasets was also calculated, and are presented in table 7.

Table 6. Results of the goodness of fit tests for the 5 first cycles as a single dataset.

Nominal value of I_1	Computed *p*-value	Computed W value	Distribution that best fits
+30 mA	0.01	0.967	None
−30 mA	0.19	0.982	Normal
+10 mA	2.9×10^{-7}	0.885	None
−10 mA	0.46	0.987	Normal
+3 mA	0.42	0.987	Normal
−3 mA	0.78	0.991	Normal
+1 mA	0.14	0.980	Normal
−1 mA	0.05	0.975	Normal
+0.3 mA	0.48	0.988	Normal
−0.3 mA	0.82	0.992	Normal

Table 7. Summary of Pearson coefficient (ρ) calculation results, second scenario, all cycles as a single dataset.

Absolute nominal value	ρ (positive current values)	ρ (negative current values)	Degree of correlation (positive values)	Degree of correlation (negative values)
30 mA	−0.87	−0.75	High	High
10 mA	0.87	0.28	High	Very low
3 mA	−0.40	−0.23	Low	Very low
1 mA	0.73	−0.77	High	High
0.3 mA	0.04	−0.15	Very low	Very low

4. Conclusion

This paper discussed the mathematical model of the CCC that is serving as a pilot study in the scope of a research project aiming at developing a virtual resistor applicable to the Metrology in Electrical Resistance Standardization. The findings presented in this work showed that the currents provided by the CCC not always fit to a normal distribution. Hence, it is always necessary to examine the data according to the scenario considered to be able to ratify the parameters of the probability distributions. Furthermore, the approximation that the current is constant throughout a measurement round cannot be assumed, given the strong correlation between the current values and time for some current ranges.

This work shall continue by refining the descriptive statistics calculations (i.e., calculating means, standard deviations, amplitudes and uncertainties for the second scenario), incorporating the noise sources to the analyses, and applying the results presented here to the models to be simulated.

References

[1] Dahono P A, Bahar Y R, Sato Y. and Kataoka T 2001 Damping of transient oscillations on the output LC filter of PWM inverters by using a virtual resistor *Proc. 4th IEEE Int. Conf. on Power Electronics and Drive Systems (Denpasar)* vol 1 (Denpasar: IEEE) p 403–407. DOI: 10.1109/PEDS.2001.975347

[2] Ogata K 2009 *Modern Control Engineering* (Upper Saddle River: Pearson)

[3] Barbosa B H G, Aguirre L A, Martinez C B and Braga A P 2011 *IEEE Trans. Control Syst. Technol.* **19**(2) 398–406

[4] NIST c2021 *NIST Uncertainty Machine.* Available at https://uncertainty.nist.gov

[5] Lafarge T and Possolo A 2015 *NCSLI Measure* **10**(3) 20–27

[6] Williams J M, Janssen T J B M, Rietveld G and Houtzager E 2010 *Metrologia* **47**(3) 167

[7] Williams J M 2011 *IET Sci. Meas. Technol.* **5**(6) 211–224

[8] Williams J M, Rietveld G, Houtzager E and Janssen T J B M 2011 *IEEE Trans. Instrum. Meas.* **60**(12) 3907–3912
[9] Marshall K, Kleinschmidt P and Williams J 2007 *Automated Cryogenic Current Comparator Bridge: Operators Manual* (*S. l.*: National Physical Laboratory)
[10] Rolland B, Stock M, Gournay P, de Oliveira V C, Carvalho H R and Landim, R P 2022 *Metrologia* **59**(1A) 01004
[11] Agilent 2012 *3458A Multimeter: User's Guide* (Loveland: Agilent Technologies, Inc.)
[12] BIPM, IEC, IFCC, ILAC, ISO, IUPAC, IUPAP and OIML 2008 *Evaluation of measurement data – Guide to the expression of uncertainty in measurement.* Available at https://www.bipm.org/documents/20126/2071204/JCGM_100_2008_E.pdf/cb0ef43f-baa5-11cf-3f85-4dcd86f77bd6
[13] Razali N M and Wah Y B 2011 Power comparisons of Shapiro-Wilk, Kolmogorov-Smirnov, Lilliefors and Anderson-Darling tests *J Stat Model Anal* **2**(1) 21–33
[14] Mukaka M M 2012 Statistics corner: A guide to appropriate use of correlation coefficient in medical research *Malawi Med J* **24**(3) 69–71. Available at https://www.ncbi.nlm.nih.gov/pmc/articles/PMC3576830
[15] de Oliveira V C, Carvalho H R and Landim, R P 2021 *J. Phys.: Conf. Ser*. **1826** 012088